



Lawrence Berkeley Laboratory

UNIVERSITY OF CALIFORNIA

Accelerator & Fusion Research Division

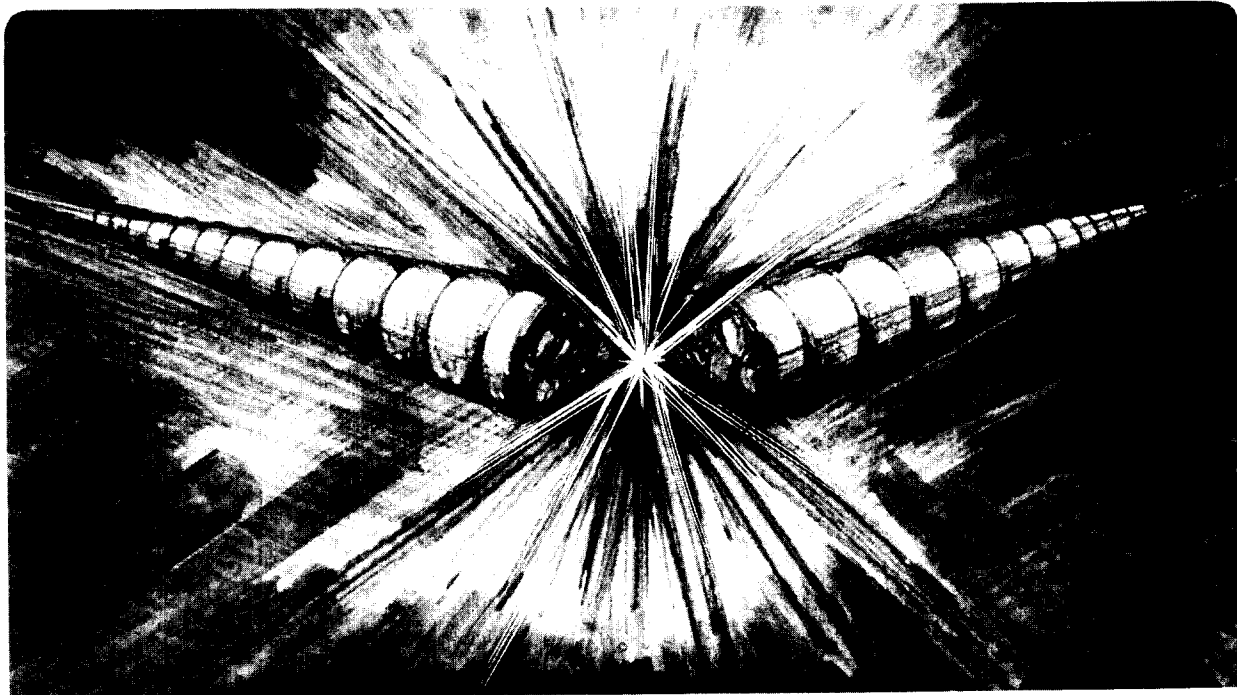
Presented at the International Symposium on Heavy Ion
Inertial Fusion, Princeton, NJ, September 6-9, 1995, and
to be published in the Proceedings

Design and Construction of a Large Aperture Quadrupole Electromagnet for ILSE

W.M. Fawley, M.C. Vella, C. Peters, M. Stuart, and A. Faltens

August 1995

509550



DISCLAIMER

This document was prepared as an account of work sponsored by the United States Government. While this document is believed to contain correct information, neither the United States Government nor any agency thereof, nor The Regents of the University of California, nor any of their employees, makes any warranty, express or implied, or assumes any legal responsibility for the accuracy, completeness, or usefulness of any information, apparatus, product, or process disclosed, or represents that its use would not infringe privately owned rights. Reference herein to any specific commercial product, process, or service by its trade name, trademark, manufacturer, or otherwise, does not necessarily constitute or imply its endorsement, recommendation, or favoring by the United States Government or any agency thereof, or The Regents of the University of California. The views and opinions of authors expressed herein do not necessarily state or reflect those of the United States Government or any agency thereof, or The Regents of the University of California.

This report has been reproduced directly from the best available copy.

Lawrence Berkeley National Laboratory
is an equal opportunity employer.

LBL-37748
UC-414

Design and Construction of a Large Aperture Quadrupole Electromagnet for ILSE

W.M. Fawley, M.C. Vella, C. Peters, M. Stuart, and A. Faltens

Accelerator and Fusion Research Division
Lawrence Berkeley National Laboratory
University of California
Berkeley, California 94720

August 1995

This work was supported by the Director, Office of Energy Research, Office of Fusion Energy, of the U.S. Department of Energy under Contract No. DE-AC03-76SF00098.

Design and Construction of a Large Aperture Quadrupole Electromagnet for ILSE*

W.M. Fawley, M.C. Vella, C. Peters, M. Stuart and A. Faltens
Lawrence Berkeley National Laboratory, Berkeley, CA 94720

Abstract

We are currently constructing a prototype quadrupole electromagnet for the proposed Induction Linac Systems Experiment (ILSE) at LBNL. ILSE will address many physics and engineering issues relevant to the design of a heavy-ion fusion driver accelerator. The pulsed electromagnet has two layers of current windings and will produce a field gradient of 28 T/m, with a usable aperture of 6 cm. It operates at a repetition rate of 1 Hz, steady-state. In this paper, we discuss how the interaction of various concerns such as maximum dynamic aperture, short lattice period, field quality, iron yoke weight, heat transfer, and voltage standoff have led to our particular design choices. We also present 2- and 3-D numerical calculations concerning field topography and the results of transport simulations of space-charge dominated ion beams with ILSE parameters.

I. Introduction

Most of the beam transport in heavy ion fusion (HIF) drivers will be done with strong-focusing, magnetic quadrupoles. In many driver designs, electrostatic quadrupoles provide focusing from the ~2 MV injector up to approximately 50-100-MV, where the transition to magnetic transport is made. The actual transition energy depends critically upon the maximum

transportable current by the magnetic quadrupole lattice which scales as $(a/L)^2 V^{3/2}$ where a is the useful dynamic aperture, L is the half-lattice period, and V is the beam energy. Thus, in the low energy portion of the magnetic transport section, there is a premium for maximizing the aperture ratio.

In the past few years, the LBL HIF group has developed a conceptual design for the 10-MV ILSE ("Induction Systems Linac Experiment") accelerator, which will allow examination of many physics and engineering issues common to HIF drivers. As part of this effort, we have designed and are currently building a large aperture, short lattice period, pulsed electromagnet prototype to be used in the 5-10-MV magnetic transport section of ILSE. The magnet must operate dependably at a continuous, 1-Hz repetition rate and transport $\approx 1-1.5 \mu\text{C/m}$ of a space-charge dominated K^{+1} beam with minimal emittance degradation. This paper presents philosophy and tradeoffs which guided the design of this magnet.

II. Basic Beam and Magnet Parameters

As presently conceived, the ILSE injector will produce four individual beams of $\sim 0.2 \mu\text{C/m}$ line charge density which will be accelerated by induction cores, slowly compressed longitudinally to perhaps as much as $0.3 \mu\text{C/m}$, and transported via electrostatic quadrupoles up to $\approx 5 \text{ MV}$ energy. At this point, the beams will be combined and merged into one single beam which then is transported magnetically to the beam dump. The half-lattice period L increases in the electrostatic transport region from 0.25 m to 0.40 m and the present beam combiner/merger design has $L = 0.5 \text{ m}$.

For a strongly space-charge dominated beam ($\sigma \ll \sigma_0$),

$$\left(\frac{a_b}{L}\right)^2 = \frac{2Q}{(1 - \cos \sigma_0)} = \frac{\lambda}{4\pi\epsilon_0 V} \quad (1)$$

where Q is the beam perveance, and σ and σ_0 are respectively the undepressed and space-charge depressed phase advance per full lattice period $2L$. If $\sigma_0 \approx 72^\circ$ at 5 MV and $\lambda = 1.5 \mu\text{C/m}$, the perveance is 2.7×10^{-3} and the required a/L is less than 0.1. Although this seems to be a comfortably small number, in fact due to longitudinal "packing factor" constraints induced by the space required for the accelerating gap, insulators, couplers, *etc.*, the magnet windings in the latest ILSE prototype design occupy only about one-half of the half-lattice period. Hence, the ratio of the winding radius to the effective length exceeds 0.2 and one must be careful to minimize anharmonic fringe field and higher order multipole components.

The required field gradient may be roughly estimated from the relation

$$\sigma_0 = \frac{v_z B' L^2}{V 2\pi} \quad (2)$$

where B' is measured in T/m and we presume that the field is dominated by the fundamental longitudinal harmonic. For 5 MV K^{+1} , $L=0.5$ m and $\sigma_0=72^\circ$, the required gradient is about 18 T/m.

A. Current Winding Geometry

To minimize anharmonic field components, we follow the philosophy of Laslett *et al.* [1] and make such components disappear in the z -integrated sense over a half-lattice period. Ignoring for the moment turn-to-turn crossovers, our actual coil ends have elliptical projections in (θ, z) space (see Fig. 1 of ref. [2]). This geometry avoids sharp bends for the individual wires. In order to limit the current per turn to 5 kA or less, the magnet has two layers of twelve turns each. Ideally, the end curve of each turn would be individually separated in z from its neighbors (to suppress the maximum number of unwanted harmonic overtones in θ), but, in practice, we found it necessary to distribute the 12 turns in each layer into 5 individual "blocks" in a 4-3-3-1-1 pattern (see Fig. 1) to obtain sufficient spacing for the cutting tool in θ between adjoining blocks (and adjacent quadrants).

Figure 1.

Figure 2.

From "engineering" constraints (see §II B and II C discussion), the iron yokes of adjoining magnets were separated approximately 13 cm in z . We have also specified that each end of the yoke should extend approximately one wire radius (8.5 cm) in z beyond the outermost coil wire in order to confine the fringe fields in z . Hence, the maximum z -length of each coil is thus ≈ 30 cm for $L=60$ cm. Setting the z -extent (2.0 cm) of the curve of each coil block end, the z -separation (1.0 cm) between adjoining blocks, and the wire diameter (0.32 cm for our particular braided copper choice), the total z length of each block and its individual wires is fully determined. The azimuthal positions of each block are then found numerically by forcing the z -integrated harmonic overtones to zero (see ref. [3] for details).

The first prototype was constructed primarily to investigate thermal heat dissipation, without detailed attention to the geometry of the wire crossovers from one block to another (which caused net dipole current loops), or, to the presence of a solenoidal loop caused by the azimuthal advance of the wire leads leaving one quadrant and entering another. In our current design, we have carefully created "X" shaped crossovers (see Fig. 1) whose projections on the θ - z plane lead to a net dipole area is less than 0.5 cm^2 for each layer of each quadrant. We have also returned the exiting wire lead of the fourth quadrant back the "long way" azimuthally to the first quadrant in order to eliminate the solenoidal loop problem. Hence, we expect a much higher quality magnetic field when we make detailed measurements of the second prototype during the next year. (see ref. [4] for details)

B. Iron Yoke Design

The first goal for the iron yoke is to increase field strength, while avoiding saturation. This maintains field quality. For a heavy ion driver, a conflicting requirement is to minimize the outer

diameter of the yoke. This reduces the inner diameter of the induction cores that surround the magnet. The cores have an annular shape, with a fixed, required cross sectional area. Hence, minimizing the I.D. of the cores reduces volume, and core cost. Reducing the outer diameter of the yoke also reduces weight, which makes support and articulation easier.

To reduce yoke diameter, the material of the yoke in the second prototype was changed to low carbon steel, which has a high saturation induction: 2.08 T as compared to 1.96 T for the 3% silicon steel used in a prototype previously constructed. We chose an inner yoke radius of 12.13 cm which is large enough to allow the magnetic fields to fall off by more than a factor of two from their values at the current windings, but does not increase magnetic core costs significantly. Taken together, these modifications reduced the effective outer yoke radius by 3 cm which translates into a projected savings of $\approx 250\text{K}$ per magnetic quadrupole section of ILSE.

We also changed the originally square cross section of the yoke to an irregular octagon by cutting off the "corners" of the yoke across from the pole of the winding. This reduces the weight of the yoke without affecting function. The octagonal shape is possible because iron saturation occurs not at near pole, but at the mid-plane, where flux is linked between neighboring poles.

The iron yoke also serves several important secondary functions. First, it minimizes magnetic fringe fields from extending greatly in z or r and interfering either with the beam transport or the induction core material (and visa versa). Second, it mechanically confines the windings and prevents their expansion and distortion under the magnetic stresses. Third, it provides a fiducial for mechanical alignment and adjustment.

C. Magnet Field Calculations

The magnet and iron yoke were designed based on 2D POISSON calculations. The design was later checked with the TOSCA 3D code. The 2D POISSON results (Fig. 2 shows the output from one example) suggest that at field gradients ≤ 26.5 T/m the maximum B-field strength in the yoke remains below 1.5 T and saturation effects are minimal. We are particularly concerned

that saturation (due to the dominant quadrupole component) might destroy the z-integrated cancellation of higher harmonics (in particular the dodecapole) within each half-lattice period. The TOSCA 3D runs indicate that, using 5.4 kA wire current, field gradients of up to 28.6 T/m at the magnet center in z are possible with minimal field leakage (≤ 10 G) radially outside the iron yoke. A 95% packing fraction was used for the iron laminations in the TOSCA runs. Both codes show that the yoke enhances the interior quadrupole field gradient by about 20%. TOSCA results have an enhanced gradient of 21% at the magnet center, with an average enhancement of 23% over the magnet length. The effective length of the quadrupole component is 0.24 m. Without enhancement from the iron yoke, a field gradient of 19.5 T/m (corresponding to 4.2 kA wire current) produced an expected $\sigma_0=72^\circ$ at 5 MV.

Axial profiles of the quadrupole and dodecapole components at a radius of 6 cm, with a current of 5.4 kA are illustrated in Figure 3, with and without iron. This corresponds to approximately 80% of the physical aperture, which is often taken as the nominal usable aperture. The 20+ percent enhancement of the quadrupole component due to the iron is obvious (Fig. 3a). The dodecapole component exhibited no corresponding enhancement at this radius (Fig. 3b) and thus, the iron yoke effectively improves magnet quality.

Figure 3a

Figure 3b

D. Mechanical Design

To meet the requirements of a heavy ion accelerator, the aperture radius was set at 75 mm, and the effective magnetic length at 249 mm, which give the magnetic an aperture radius about 1/3 the effective coil length. One prototype has been constructed and tested; a second prototype is under construction. In the first prototype, we concentrated our design efforts on creating a magnet

that would be electrically and mechanically reliable over the long-term. In the second prototype, we refined the design to improve magnet quality.

The magnet consists of a coil form, the conductors, electrically insulating-heat conducting epoxy, cooling passages, and a flux return yoke (See figure 4). The coil form is a plastic cylinder onto which elliptically ended, "race-track" shaped grooves were numerically machined to position the conductor cables. The quadrupole has 24 turns per pole, arranged in two layers. This allows 130 kA-turns per quadrant, corresponding to a peak field in the coils over 2 Tesla. Rectangular, litz wound cable is used as a conductor to minimize eddy current losses. After winding the conductor onto the coil form, the assembly was vacuum potted with thermally conductive epoxy. A 3 mm layer of epoxy was left outside the conductors and coil form to provide electrical insulation between the conductors and water coolant. A cooling jacket was made by stacking a number of PVC rings, which had steps and offset holes cut into them to provide a water passage. The rings are slid over the potted windings, as illustrated in figure 5. The I.D. of the PVC rings provides an interference fit with the outside of the potted magnet. The whole assembly was then potted into a yoke constructed of steel laminations.

Figure 4.

Figure 5.

Electrical reliability requires minimizing the voltage across the leads, and providing adequate insulation between the cables and cooling. The magnet was vacuum potted, then cured under one atmosphere of pressure to minimize bubbles. This reduces the chance of plasma forming in pockets within the epoxy. The conductor cross section was dictated by consideration of breakdown, magnet heating and ease of winding. The relationships of conductor size, power dissipation, lead voltages, and number of turns per quadrant of the magnet are shown in figure 6. This figure also illustrates the fact that the total conductor area must be at least 55% of the cross section to obtain correct spacing for the required $\cos 2\theta$ current distribution.

Figure 6.

A reasonable conductor size to optimize power, voltage, and windability would be a 3 x 5 mm stranded conductor. In the first prototype, 3.2 x 6.4 mm litz twisted cable constructed of 7, 14 gauge copper wire was used, with 24 turns per quadrant. At the required current of 5400 A, the voltage across the leads was 10.8 kV. Thermal modeling (which assumed a 1.1 kW power loss in the conductors) showed a temperature gain from outside to inside of about 40°C and a maximum inner conductor temperature of 60°C. In the second prototype, the original, stiff conductor was replaced by a more flexible conductor with the same overall cross sectional area, to meet the more stringent bending requirements necessary for improving the magnetic field quality. The "new" cable was also litz twisted, with 7 bundles of 13 strand, 26 gauge wire. Although the overall cross sectional area of the second conductor remained the same as the first, the actual current carrying area of the cable was reduced by 20%. This requires higher currents, and causes the temperature differential between the water and the inner cable to increase to 55°C for the outer winding, and 75°C for the inner winding.

The design of the second prototype magnetic quadrupole was directed towards manufacturing a magnet with the field quality that will eventually be necessary for focusing a beam of heavy ions in a linear accelerator from an energy of 5 MeV to 10 MeV. The two features of the previous magnet that needed improvement were the path that the conductors took when crossing from one "race-track" across to another, and removing the effective solenoid loop created by the connection of the cable leads at the end of the magnet. (See ref [4] for details.)

III. Particle Simulation Studies

We have used the 2D particle simulation code "HIFT" [3] to model the transport dynamics of a 1.5 $\mu\text{C}/\text{m}$ space-charge dominated 5-MV, K^{+1} beam through 24 m of magnetic transport (without acceleration gaps). The model magnetic fields included the quadrupole, dodecapole,

pseudo-octupole, and pseudo dodecapole components scaled from a 3D field solution which did not include the effects of the iron yoke. The peak field gradient at the center of each magnet was set to 19.5 T/m giving an undepressed phase advance σ_0 of 72 degrees per lattice period. The normalized edge emittance of the beam was set to 5π mm-mrad which gave to a space-charge depressed tune σ of approximately 7 degrees. The beam was initialized with a KV distribution in transverse phase space which led to a maximum beam envelope extent of 69 mm as compared with a presumed beam pipe radius of 75 mm. Over the 20 lattice periods, no simulation particles were lost and the emittance growth was of order 5% or less. Consequently, we are confident that, if the magnet performs according to design, it will be able to transport the specified beam line charge without serious degradation.

Acknowledgement

*This work was supported by the Director, Office of Energy Research, Office of Fusion Energy, U.S. Dept. of Energy, under Contract No. DE-AC03-76SF00098.

FIGURE CAPTIONS

Figure. 1. Artist's depiction of the projected coil turn geometry of the quadrupole magnet prototype.

Figure. 2. 2D POISSON results showing the field line topology in the r - θ plane of an octant of the quadrupole magnet plus iron yoke. The midplane field gradient at $r=0$ was 26.5 T/m. The peak field in the iron yoke is 1.5 T/m

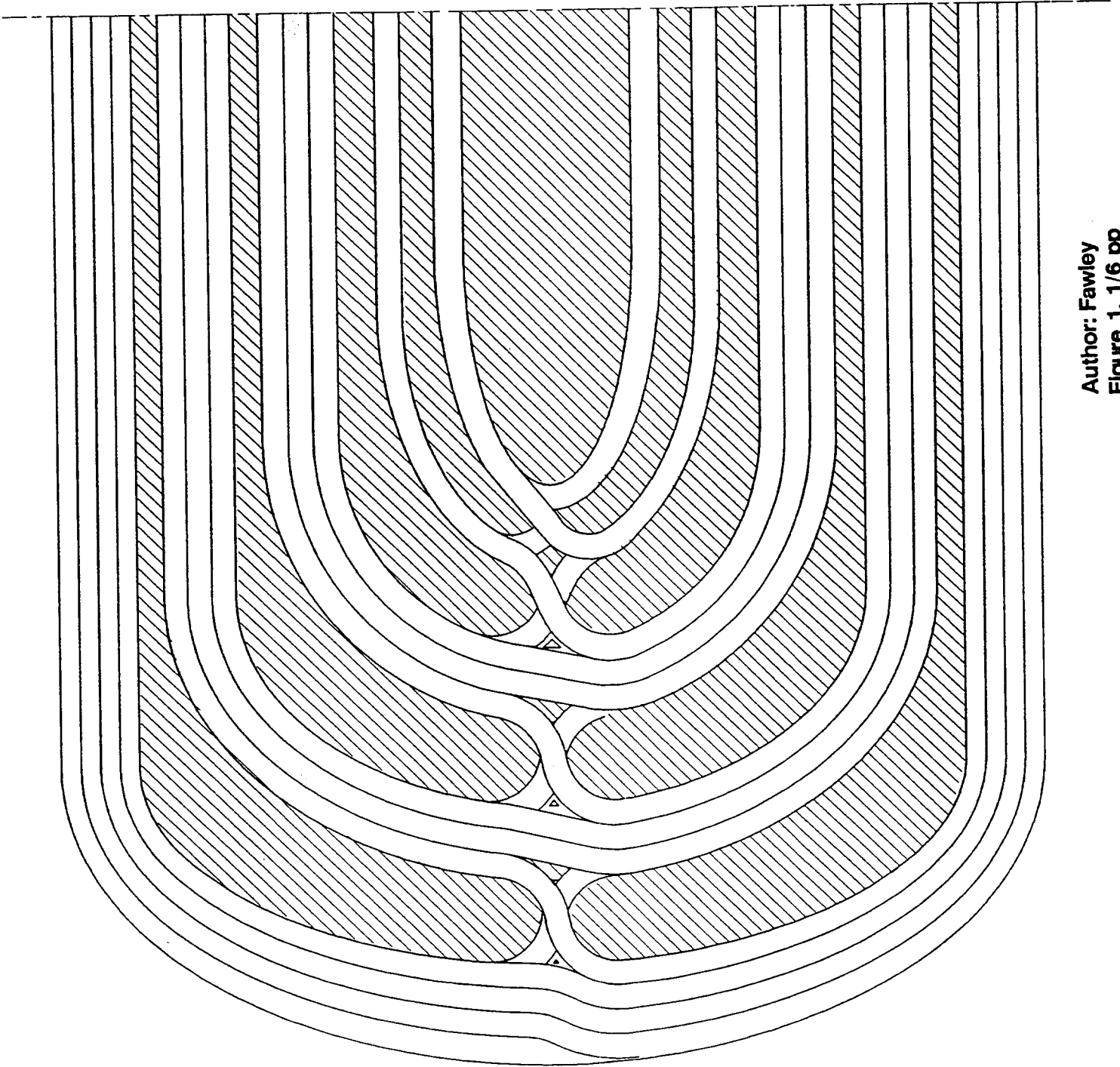
Figure 4. Cross-sectional view of one quadrant of the Magnet

Figure 5. The Magnetic Quadrupole Cooling Jacket

Figure 6. Conductor size versus energy loss

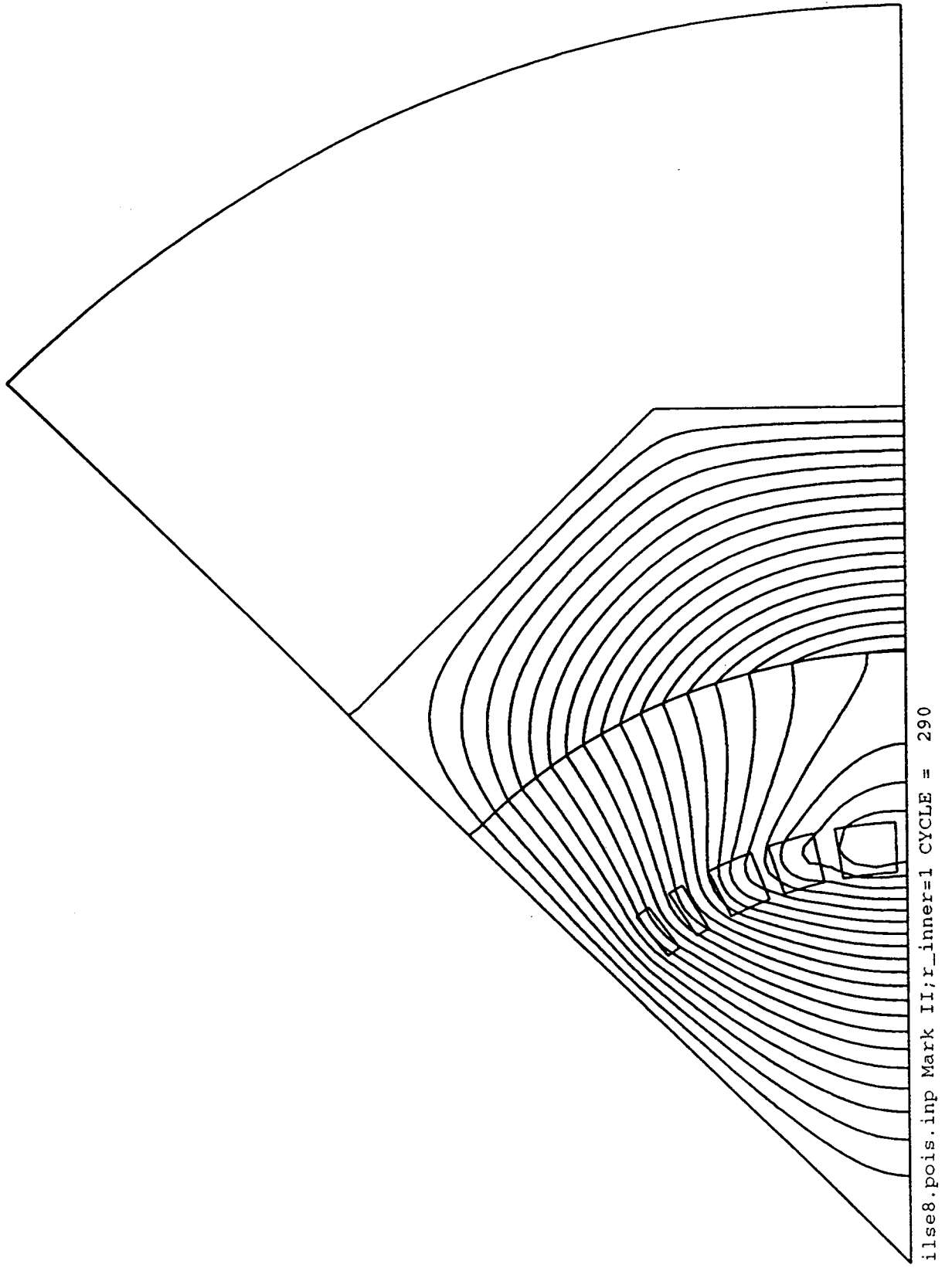
REFERENCES

- [1] Laslett, L.J., Caspi, S., and Helm, M., *Particle Accel.*, **22**, 1 (1987)
- [2] Fawley, W.M., Laslett, L.J., Celata, C.M., Faltens, A., and Haber, I., "Simulation Studies of Space-Charge-Dominated Beam Transport in Large Aperture Ratio Quadrupoles", *Proceedings of the 1993 IEEE Particle Accelerator Conference*, **93CH3279-7**, 724 (1993).
- [3] Fawley, W.M., "Space-dominated Beam Transport in Magnetic Quadrupoles with Large Aperture Ratios", **LBL-33608**, 1993.
- [4] Reginato, L., Faltens, A., Fawley, W., Peters, C., Stuart, M., Benjegerdes, R., "Design and Testing of the Magnetic Quadrupole for the Heavy Ion Fusion Program", presented to the 1995 Particle Accelerator Conference, Dallas, Texas, May 1995.

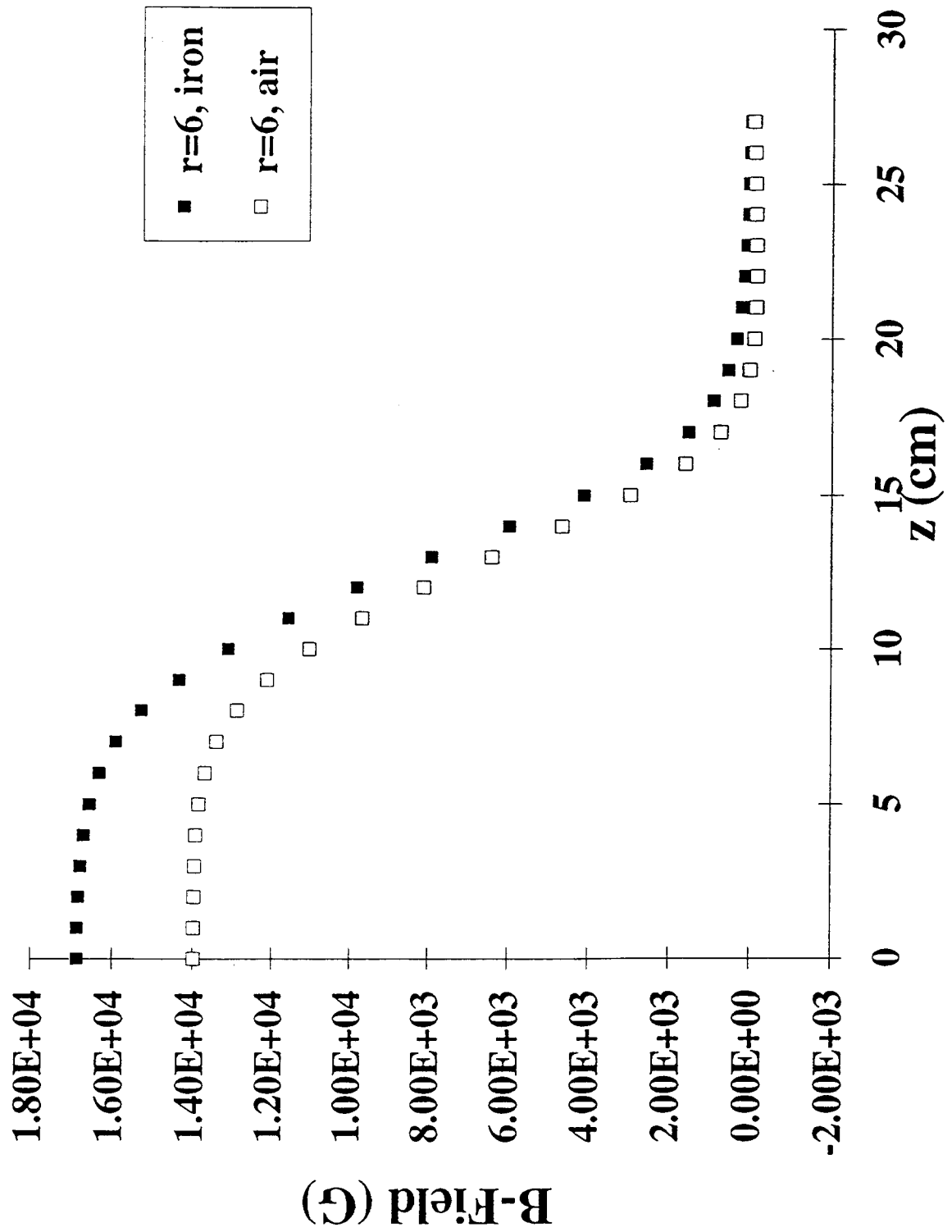


Author: Fawley
Figure 1, 1/6 pp

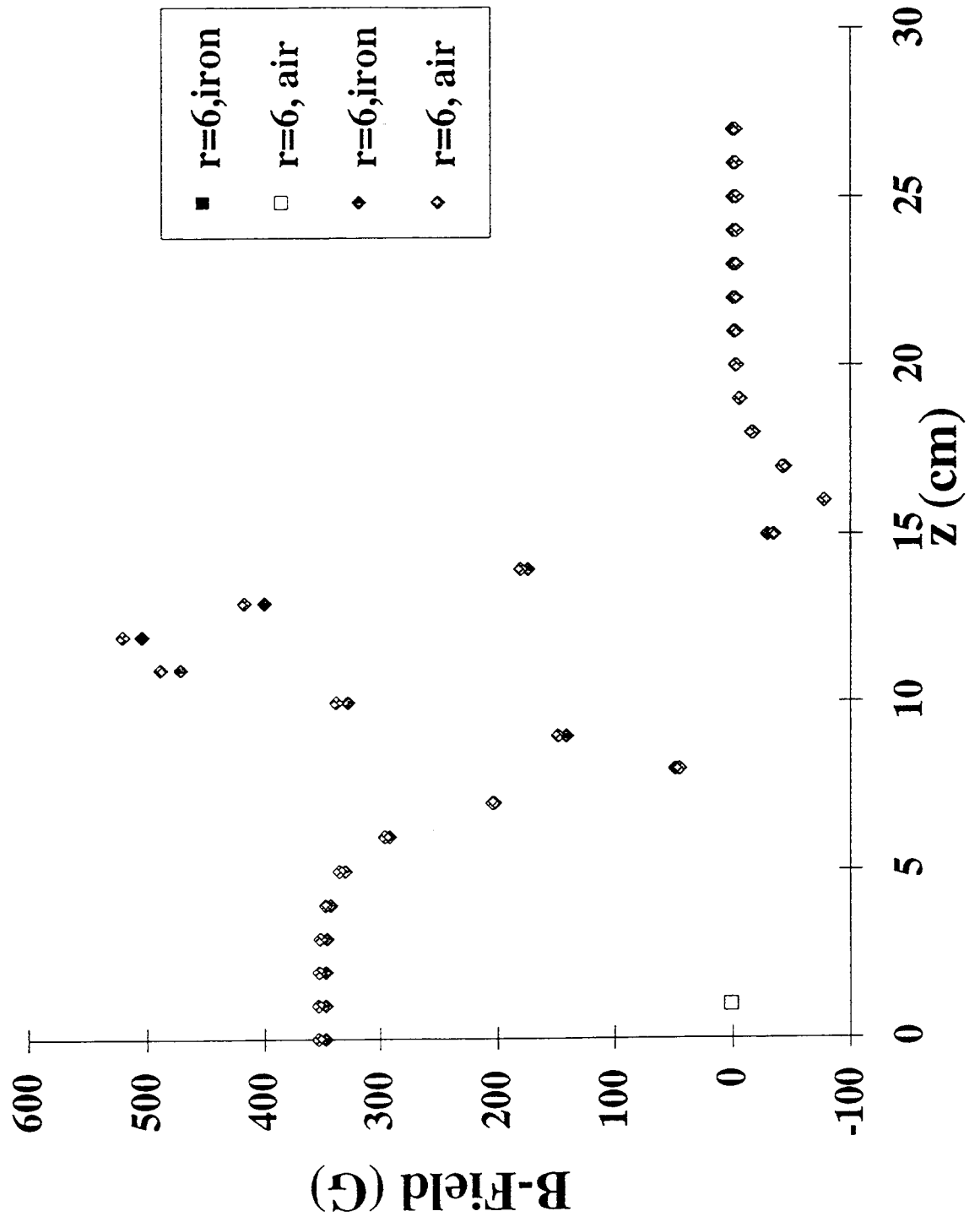
Author: Fawley
Figure 2, 1/6 pp

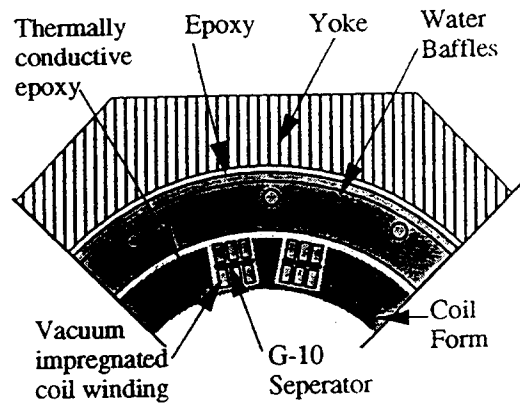


Author: Fawley
Figure 3a, 1/6 pp

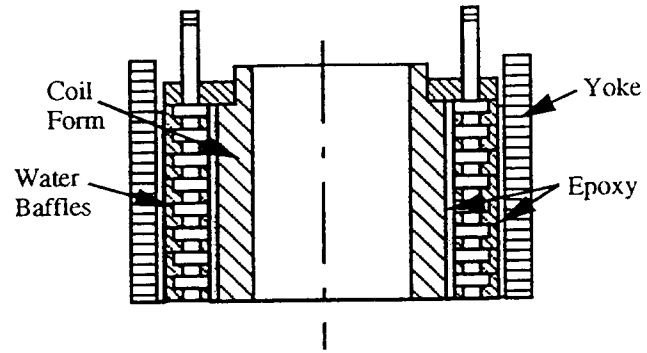


Author: Fawley
Figure 3b, 1/6 pp

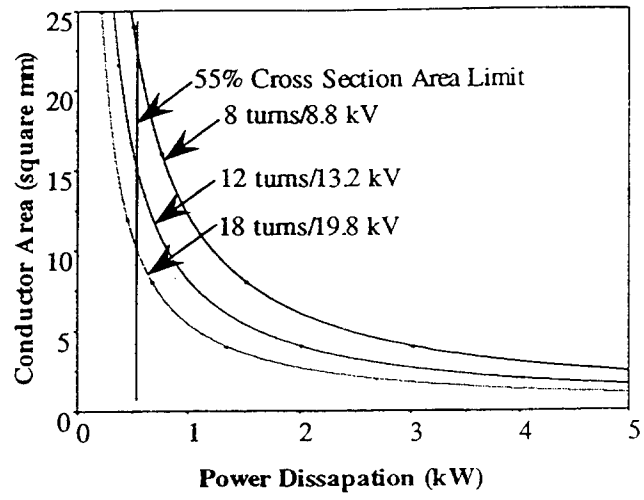




Author: Fawley
Figure 4, 1/6 pp



Author: Fawley
Figure 5, 1/6 pp



Author: Fawley
Figure 6, 1/6 pp